

## Chemisorption of pyrrole and polypyrrole on Si(001)

K. Seino,\* W. G. Schmidt, J. Furthmüller, and F. Bechstedt

*Institut für Festkörperteorie und Theoretische Optik, Friedrich-Schiller-Universität Jena, Max-Wien-Platz 1, D-07743 Jena, Germany*

(Received 1 September 2002; revised manuscript received 28 October 2002; published 31 December 2002)

The functionalization of the Si(001) surface by pyrrole and polypyrrole is investigated by means of *first-principles* pseudopotential calculations. We find dissociative reactions, leading to the partial fragmentation of the molecule, to be energetically most favored for pyrrole adsorption. The lowest energy configuration for monolayer coverage is characterized by pyrrole rings bonded to the surface via Si-N linkage. In co-existence with alternative adsorption geometries where both N and C are bonded to the surface, this structure accounts very well for the available experimental data. Chemisorption of pyrrole is found to effectively passivate the Si(001) surface, irrespective of the details of the adsorption geometry. The formation of well-ordered polypyrrole structures on Si(001) may require chemical modifications of the polypyrrole chains in order to accommodate the lattice mismatch-induced strain.

DOI: 10.1103/PhysRevB.66.235323

PACS number(s): 68.43.Bc, 68.35.Md

### I. INTRODUCTION

Organic molecular adsorption on semiconductor surfaces has become important for semiconductor-based devices with novel properties.<sup>1–3</sup> Examples include thin-film displays, molecular electronics, as well as chemical and biological sensors. Because of the widespread use of Si in microelectronics, the formation of well-ordered organic thin films on the Si(001) surface is of particular importance. Additionally, such systems are of interest from a surface science point of view: the silicon dimers of the reconstructed Si(001) surface, forming a strong  $\sigma$  and a weak  $\pi$  bond, allow for a series of interesting surface reactions. Recent experimental and theoretical investigations have shown some analogies between the reactivity of the silicon dimers and the reactivity of unsaturated organic molecules.<sup>1,3–10</sup> For example, the adsorption of alkenes may proceed by utilizing the two electrons from the  $\pi$  bond of the silicon dimer and two electrons from the  $\pi$  bond of the C=C group for the formation of two new C-Si  $\sigma$  bonds. The surface reaction with bifunctional organic molecules may allow for creating an ordered array of possible further reaction sites, provided the second functional group remains intact. Molecules containing nitrogen have found particular attention in this respect: the amine group may be used for the attachment of biomolecules such as DNA to the surface.<sup>11</sup>

Pyrrole (C<sub>4</sub>H<sub>4</sub>NH, cf. Fig. 1) is an example for a molecule containing both unsaturated carbon bonds and nitrogen. Here nitrogen is part of a five-member aromatic ring. Qiao *et al.*<sup>12</sup> reported the formation of a robust pyrrole monolayer on Si(001) upon direct exposure of the surface to the molecules. Based on high-resolution electron energy-loss spectroscopy (HREELS) and x-ray photoelectron spectroscopy (XPS) data, they suggested that pyrrole reacts with the surface through the cleavage of the N—H group, forming a Si—N linkage between the substrate and the pyrrole ring (structure HD in Fig. 2). Upon annealing the pyrrole assembled silicon surfaces to 500 K, the surface order is significantly enhanced. The pyrrole rings seem to be preserved for temperatures up to 700 K. Fourier transform infrared (FTIR) spectra measured by Cao and co-workers<sup>13</sup> using iso-

topically labeled compounds indicate that in addition to N—H bond cleavage, also some C—H bonds break upon pyrrole adsorption. The suggested structure corresponds to the CN1 geometry in Fig. 2.

It is known that conjugated dienes can react with the Si(001) surface via [2+2] cycloaddition and [4+2] Diels-Alder reactions.<sup>3</sup> The pyrrole molecule possibly adsorbs on Si(001) also via these two reactions. [2+2] and [4+2] reactions as well as the HD adsorption configuration have been studied by Luo and Lin<sup>14</sup> using cluster calculations.

Polymerized pyrrole shown in Fig. 1 is a good organic conductor.<sup>15</sup> It may therefore represent an alternative to the formation of organic nanowires consisting of relatively large molecules such as diacetylene.<sup>16</sup> In addition, polypyrrole covered silicon surfaces are used for “gene tip” technologies, where biological information is gained using polypyrrole DNA chips.<sup>17</sup>

Here we present a comprehensive study on the adsorption of pyrrole and polypyrrole on Si(001) surfaces based on *first-principles* total-energy calculations for periodic supercells.

### II. COMPUTATIONAL METHOD

The total-energy and electronic-structure calculations are performed using the Vienna Ab-initio Simulation Package (VASP) implementation<sup>18</sup> of the gradient-corrected<sup>19</sup> density functional theory (DFT-GGA). The electron-ion interaction is described by non-normconserving ultrasoft pseudopotentials,<sup>20</sup> allowing for the accurate quantum-

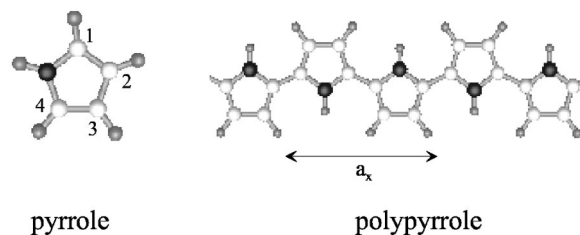


FIG. 1. Schematic drawings for pyrrole and polypyrrole. Black (white, grey) balls represent N (C, H) atoms.

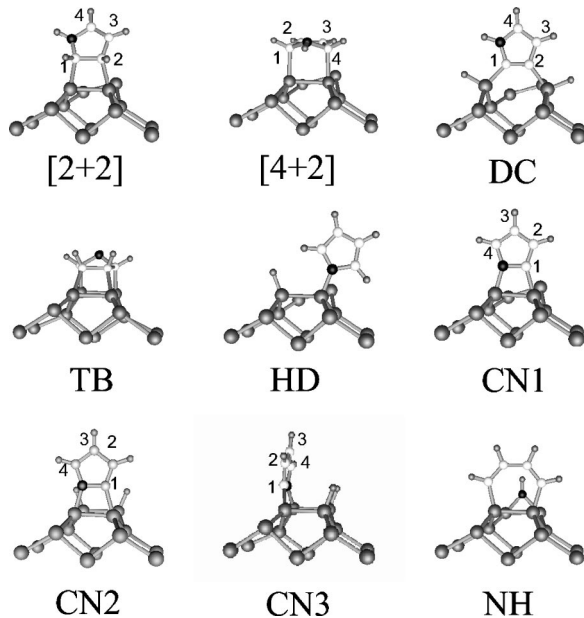


FIG. 2. Si(001):pyrrole adsorption configurations discussed in the text: products of  $[2+2]$  cycloaddition and  $[4+2]$  cycloadditions, dimer cleaved (DC), tight-bridge (TB), hydrogen dissociated (HD), C—H and N—H dissociation (CN1) and C—H and N—H dissociation with adsorbed hydrogen (CN2 and CN3), and N—H group dissociated (NH) structures. Black (white, grey) balls represent N (C, Si) atoms. Hydrogens are indicated by small symbols.

mechanical treatment of first-row elements already with a relatively low cutoff energy.

We performed extensive convergence tests on the gas-phase pyrrole molecule using a  $11 \times 11 \times 11 \text{ \AA}^3$  supercell. The total energy and characteristic bond lengths are found to be completely converged (and the latter in excellent agreement with experiment) for a cutoff energy of 30 Ry (cf. Fig. 3). This value has been used throughout the calculations. For polypyrrole (PPy) we determine an equilibrium lattice constant  $a_x = 7.17 \text{ \AA}$  (cf. Fig. 1). The separation between the highest occupied molecular orbital (HOMO) and lowest unoccupied molecular orbital (LUMO) decreases with increasing chain length.<sup>21</sup> We calculate HOMO-LUMO gaps of 4.34, 3.28, and 1.97 eV for the monomer, bipyrrrole, and PPy, respectively (experiment<sup>21</sup>: 5.96, 4.35, and 3.0 eV). For bulk Si we determine an equilibrium lattice constant of 5.456 Å, a bulk modulus of 0.879 Mbar, and a fundamental energy gap of 0.64 eV (experiment<sup>22</sup>: 5.43 Å, 0.96–0.99 Mbar, and 1.17 eV). The slight overestimation of the lattice constant as well as the slight underestimation of the bulk modulus and the failure to reproduce the band gap are typical for DFT-GGA calculations.

The functionalized Si(001) surface is modeled with a periodically repeated slab. The supercell consists of eight atomic Si layers plus adsorbed molecules and a vacuum region equivalent in thickness to 12 atomic layers. The Si bottom layer is hydrogen saturated and kept frozen during the structure optimization. All calculations are performed using the calculated Si equilibrium lattice constant. Depending on the molecule coverage investigated, supercells with  $(4 \times 2)$ ,  $(2 \times 2)$ , or  $(2 \times 1)$  surface periodicity are used. The topmost

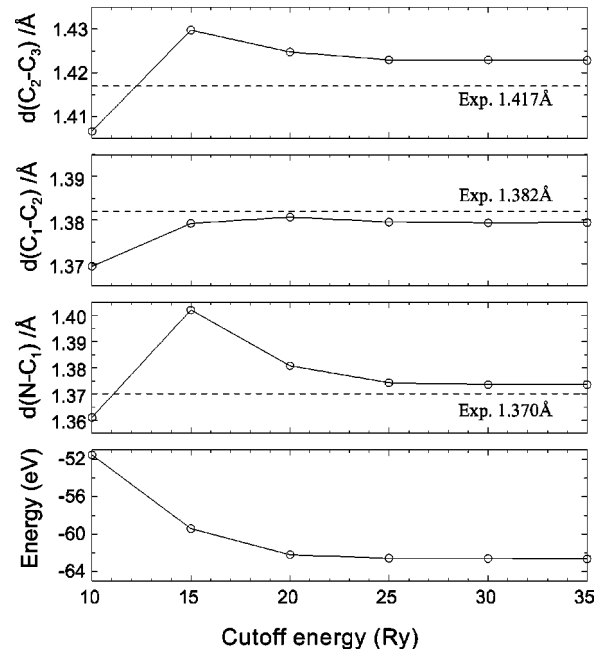


FIG. 3. Equilibrium bond lengths and total energy of gas-phase pyrrole vs the plane-wave cutoff energy. The experimental data are taken from Ref. 23.

five layers of the slab as well as the adsorbed molecules are allowed to relax.

Our calculations employ the residual minimization method—direct inversion in the iterative subspace (RMM-DIIS) algorithm<sup>24,25</sup> to minimize the total energy of the system. The surface structure is considered to be in equilibrium when the Hellmann-Feynman forces are smaller than 10 meV/Å. The Brillouin-zone integrations are performed using sets corresponding to 64 **k** points in the full  $(1 \times 1)$  surface Brillouin zone.

### III. RESULTS AND DISCUSSION

#### A. Pyrrole on Si(001)

##### 1. Chemisorption structures

There exist a large number of conceivable Si(001):pyrrole interface geometries. We examined 23 models, the most relevant ones are shown in Fig. 2.

Earlier studies on various hydrocarbons have shown that  $[2+2]$  cycloadditions are facile reactions for the adsorption on Si(001).<sup>3</sup> To account for the different resonance states of pyrrole [cf. Fig. 4(a)] we consider two possibilities for a  $[2+2]$  cycloaddition reaction of pyrrole with the Si dimers, leading to either the  $[2+2]$  or the CN1/CN2 models in Fig. 2.

The structural parameters of the relaxed  $[2+2]$  structure are given in Table I. The  $C_1-C_2$  bond length parallel to the Si dimer is 1.56 Å, considerably larger than in the pyrrole molecule (1.38 Å from our calculation). This indicates the transition from a C=C double to a C—C single bond characteristic for cycloaddition reactions: the  $\pi$  bonds of the molecule and of the silicon dimer are broken and replaced by

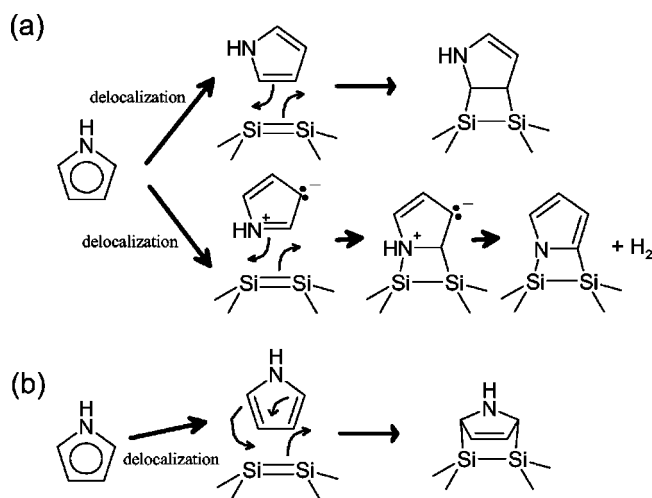


FIG. 4. Schematic illustrations of possible cycloaddition reactions of pyrrole with the Si(001) surface dimers: (a) [2+2] cycloadditions, (b) [4+2] Diels-Alder reaction.

two  $\sigma$  bonds between the molecule and the Si surface atoms. From the bond lengths in Table I, we can also see that the [2+2] cycloaddition leads to a 2-pyrroline-like structure. For the [2+2] cycloaddition, two dimerized and dimer-cleaved interface configurations with different isomers are conceivable. This is discussed in detail in our previous work.<sup>26</sup>

A [4+2] Diels-Alder reaction between pyrrole and the Si-Si dimer involves both molecular double bonds as shown in Fig. 4(b). A 3-pyrroline-like adsorption configuration is formed, as can be seen from the structural parameters in Table I. The Si dimer length is elongated to 2.37 Å (it amounts to 2.35 Å at the clean surface) and the C<sub>2</sub>—C<sub>3</sub> bond length is shortened to 1.35 Å, slightly larger than an isolated C=C double bond. The structural parameters for [2+2] and [4+2] cycloadditions agree with previous cluster calculations.<sup>14</sup>

We also investigate the possibility that the two hydrogen atoms originally bonded to the C=C group are transferred to the Si dimer atoms, facilitating the cleavage of the Si dimer (DC in Fig. 2, structural parameters in Table I). This geom-

etry is being discussed for the adsorption of the structurally similar cyclopentene molecule on Si(001).<sup>9,10</sup> The formation of “tight bridges” (TB in Fig. 2), similar to those formed by benzene on Si(001),<sup>1,4–6</sup> is a further adsorption geometry considered here. It could result from the bonding of the C=C double bond remaining after a [4+2] Diels-Alder reaction with the neighboring Si dimer.

In addition to reactions which leave the pyrrole molecule intact, we study dissociative absorption processes, where C<sub>4</sub>H<sub>4</sub>N and H bond to different surface dimers or to different dimer atoms, as suggested from experiment.<sup>12,13</sup> The Si—N distance of the HD structure shown in Fig. 2 amounts to 1.76 Å and the Si—Si—N angle is 110.1°. The C<sub>4</sub>H<sub>4</sub>N ring fragment retains the planar geometry and the aromaticity of the pyrrole molecule.

The CN1 structure shown in Fig. 2 was suggested by Cao *et al.* on the basis of FTIR data.<sup>13</sup> It results from a [2+2] cycloaddition as shown in the lower part of Fig. 4(a). In the CN2 case the two released hydrogen atoms are assumed to bond to the neighboring Si dimer. A bridging of the Si dimers is modeled with the CN3 geometry. A similar structure was found favorable for acetylene adsorbed on Si(001).<sup>7,8</sup> Structural parameters for the CN1, CN2, and CN3 structures are given in Table I. In all three cases we find the Si—N bond length to be shorter than Si—C bond length and the adsorbed molecules to retain their aromaticity.

One more dissociative reaction studied is the dissociation of the N—H group (model NH in Fig. 2). It results in a C=C—C=C bonded six-member ring and the co-adsorption of the released N—H group at another Si dimer, forming a Si<sub>2</sub>N triangle. The Si—N and N—H bond lengths are 1.74 and 1.01 Å, respectively. Similar configurations were suggested for thiophene (C<sub>4</sub>H<sub>4</sub>S) and furan (C<sub>4</sub>H<sub>4</sub>O) adsorbed on Si(001) (Ref. 27).

## 2. Energetics

The adsorption energies for the interface geometries discussed above are summarized in Table II for various coverages. Here 1 ML is defined as one molecule adsorbed per Si dimer. The varying coverage dependence of the adsorption energies leads to a different ordering of the minimum energy

TABLE I. Structural parameters for several of the geometries in Fig. 2 calculated for a coverage of 0.25 monolayers (ML). The values are compared with results for gas-phase pyrrole, 2-pyrroline and 3-pyrroline molecules. The labeling of the atoms refers to Fig. 2.

	[2+2]	[4+2]	DC	CN1	CN2	CN3	Pyrrole	2-pyrroline	3-pyrroline
Si-Si (Å)	2.36	2.37	3.80	2.37	2.37	2.39			
Si-C (Å)	2.00	2.01	1.84	1.87	1.86	1.88			
Si-N (Å)				1.78	1.80	1.81			
C <sub>1</sub> -C <sub>2</sub> (Å)	1.56	1.49	1.40	1.38	1.38	1.39	1.38	1.55	1.50
C <sub>2</sub> -C <sub>3</sub> (Å)	1.48	1.35	1.43	1.42	1.42	1.41	1.42	1.51	1.33
C <sub>3</sub> -C <sub>4</sub> (Å)	1.35	1.49	1.38	1.39	1.39	1.38	1.38	1.34	1.50
C <sub>1</sub> -N (Å)	1.44	1.46	1.38	1.42	1.42	1.43	1.37	1.48	1.47
C <sub>4</sub> -N (Å)	1.39	1.46	1.36	1.37	1.37	1.38	1.37	1.40	1.47
Si-H (Å)					1.49	1.49			
Si-Si-C (°)	79.2	90.4	49.0						

TABLE II. Calculated adsorption energies in eV/molecule for pyrrole on Si(001) for various coverages. The values refer to the  $c(4 \times 2)$  reconstructed surface ground state of Si(001). The hydrogen chemical potential corresponds to  $H_2$  at zero temperature. The notation of the geometries refers to Fig. 2.

Geometry	0.25 ML	0.5 ML	1 ML
[2+2]	0.71		0.32
[4+2]	1.19		-0.40
DC	2.02		1.36
TB	1.45	1.27	
HD	2.02	1.93	1.90
CN1	1.06		0.71
CN2	3.17	2.97	
CN3	3.00	2.79	
NH	2.57	2.37	

structures depending on the number of molecules adsorbed. For coverages up to half a monolayer, the N—H and C—H bond cleavage accompanied by the co-adsorption of the released hydrogen atoms, i.e., the CN2 and CN3 structures (cf. Fig. 2) are the most favored geometries. The HD structure is the most stable geometry for monolayer coverage.

For all structures considered, we observe a decrease in the adsorption energy as the coverage is increased, indicating a repulsive interaction between the adsorbed molecules. This is particularly obvious in case of the [4+2] Diels-Alder reaction. The repulsive interaction between the adsorbed pyrrole molecules also governs the translational symmetry. For example, the monolayer coverage for the HD structure can be achieved by arranging the molecules in a  $(2 \times 1)$  or in a  $p(2 \times 2)$  symmetry, i.e., at alternating dimer atoms. The latter symmetry is energetically slightly preferred, by 0.01 eV per pyrrole molecule.

Due to the varying surface stoichiometry, the total energies of the investigated structures are not sufficient to determine the surface ground state in some cases. The values cited in Table II refer to the situation that the surface is in equilibrium with molecular hydrogen at  $T=0$ . For more general situations, the thermodynamic grandcanonical potential  $\Omega$  in dependence on the chemical potentials  $\mu$  of pyrrole and H needs to be considered,<sup>28</sup>

$$\Omega = E - TS - n_{pyr}\mu_{pyr} - n_H\mu_H, \quad (1)$$

where  $n_{pyr}$  and  $n_H$  are the number of pyrrole and hydrogen molecules, respectively. For the actual calculations, we neglect the entropy contribution to  $\Omega$ . The energies are calculated with respect to the fully relaxed  $c(4 \times 2)$  ground state of the Si(001) surface. The calculated surface phase diagram is shown in Fig. 5. Here zero chemical potentials correspond to the situation where the surface is exposed to molecular hydrogen and pyrrole molecules at  $T=0$ .

The surface phase diagram will change for higher temperatures, due to vibrational contributions to the energy and entropy of the surface structures, and due to the temperature (and pressure) dependence of the chemical potentials of pyrrole and hydrogen. In particular the hydrogen chemical po-

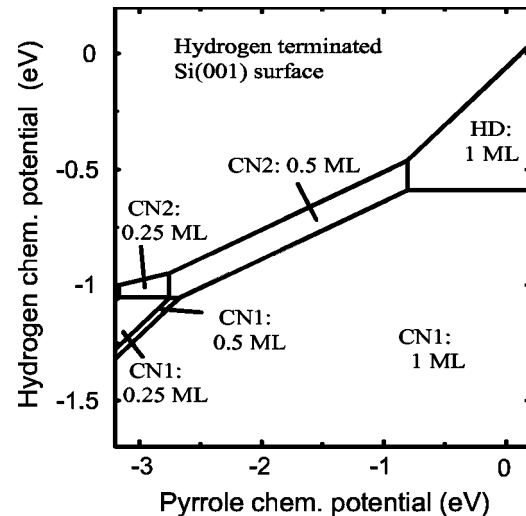


FIG. 5. Calculated phase diagram of the hydrogen- and pyrrole-exposed Si(001) surface. The notation of the structural models refers to Fig. 2. The chemical potentials of hydrogen and pyrrole are given with respect to molecular hydrogen and gas-phase pyrrole at  $T=0$ .

tential is lowered by increasing the temperature, i.e., less energy is gained by taking a hydrogen atom out of the reservoir and attaching it to the surface. It can be approximated by that of an ideal gas.<sup>29</sup> On the other hand, the hydrogen chemical potential may become larger than zero if atomic hydrogen is available. According to the calculated phase diagram, three structures may occur: sufficient supply of hydrogen and pyrrole stabilizes the HD structure in Fig. 2. If less hydrogen is available, the CN1 structure is favored. The ground state of pyrrole-deficient surfaces exposed to hydrogen, finally, is characterized by the CN2 structure.

Based on XPS peak area analysis, it was estimated that pyrrole molecules are attached to 92% of the Si surface dimers after the formation of the ordered overlayer.<sup>12</sup> For this coverage our calculations indicate that the HD structure is most favored. This structure is consistent with the experimental observations of the appearance of Si—H and Si—N stretch modes, the disappearance of the N—H stretch modes and the preservation of the pyrrole ring structure.<sup>12</sup> In a later experimental work<sup>13</sup> it was pointed out that also some C—H bond cleavage occurs during the formation of the pyrrole overlayer. The CN2 model and, although energetically less favored, the CN3 structure, are likely candidates to explain these observations. Moreover, the co-adsorption of hydrogen may explain why no full monolayer coverage has been reached experimentally. The CN1 structure is favored for hydrogen-poor conditions as can be seen from the surface phase diagram. However, the CN1 structure cannot explain the appearance of the Si—H stretching vibration. Therefore this structure is in accord with the experiments only, if a co-existence with the other chemisorption models is assumed. The experimental results and the calculated surface energies thus indicate a co-existence of adsorption geometries, with the lowest-energy configuration for high coverages of pyrrole, HD, dominating.

The interface structures actually formed do not only de-



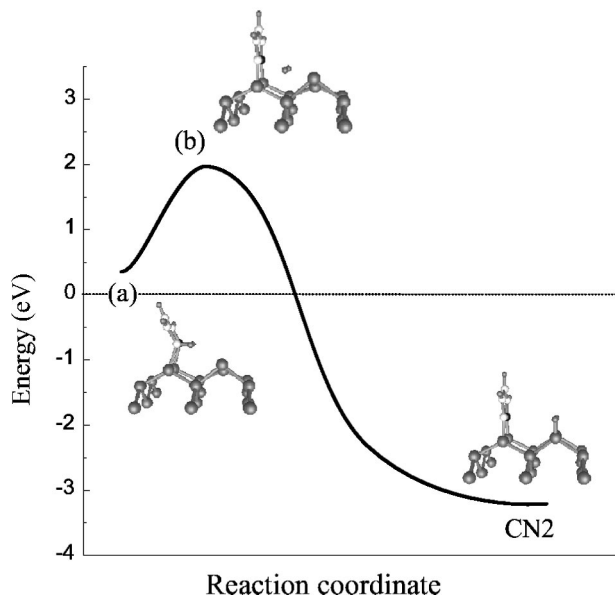


FIG. 6. Reaction energetics for the CN2 structure. The reaction coordinate corresponds to the simultaneous diffusion of two hydrogen atoms from the molecule to the neighboring Si dimer. The dotted line gives the energy of the pyrrole molecule in gas phase.

pend on the total energies, but also on the energy barriers which need to be overcome for the respective surface reactions. Our investigation of the surface reaction pathways focuses on the three low-energy structures HD, CN2, and NH. Assuming that the dissociative reaction leading to HD is analogous to the Si surface reaction with  $\text{NH}_3$ ,<sup>30</sup> Luo and Lin<sup>14</sup> investigated its reaction path using a cluster method. Our calculations using a periodic supercell yield for this process an energy barrier of 0.08 eV, much smaller than the cluster result of 0.38 eV. A similar trend of overestimated energy barriers in cluster calculations has already been found by Penev *et al.* in their systematic study on the  $\text{H}_2$  desorption and dissociative adsorption on Si(001).<sup>31</sup>

To calculate the energy barrier leading to the CN2 structure we start from the intermediate state (a) shown in Fig. 6, because the [2+2] cycloaddition leading to this state is characterized by a very small barrier.<sup>14</sup> Assuming a simultaneous diffusion of the hydrogen atoms from the pyrrole molecule to the neighboring Si dimer [state (b) in Fig. 6], we calculate an energy barrier of 1.68 eV to form the interface structure CN2. For this calculation the coordinates of the two diffusing hydrogen along the dimer row direction were kept fixed, whereas their coordinates perpendicular to the dimer row as well as the positions of the other pyrrole and Si surface atoms were allowed to relax.

The decomposition, which leads via abstraction of the N—H group to the interface structure NH, is the third reaction path considered. Starting from the [4+2] cycloaddition product the calculated activation energy amounts to 0.30 eV. This is somewhat lower than the barrier of 0.69 eV obtained for the corresponding surface reaction with furan.<sup>27</sup>

In Table III the activation energies for three interface reactions are compiled. The reaction rate for the thermally activated processes is estimated using the Arrhenius relation

TABLE III. Activation energies and hopping times at different temperatures for the assumed surface reactions leading to the HD, CN2, and HD structures (see text).

structure	$E_a$ (eV)	$\tau$ (s)@150 K	$\tau$ (s)@300 K	$\tau$ (s)@600 K
HD	0.08	$5 \times 10^{-12}$	$2 \times 10^{-13}$	
CN2	1.68		$2 \times 10^{14}$	1.3
NH	0.30	$4 \times 10^{-5}$	$4 \times 10^{-10}$	

$R = \nu_0 e^{-E_a/kT}$ , where  $E_a$  is the activation energy,  $k$  the Boltzmann constant,  $T$  the temperature, and  $\nu_0$  is the prefactor. Because the surface reactions leading to the interface structures HD and CN2 are mainly governed by the diffusion of hydrogen atoms on the surface, a prefactor  $\nu_0 = 10^{13} \text{ s}^{-1}$  typical for hydrogen diffusion on Si(001) (Ref. 32) has been chosen to calculate the hopping time,  $\tau = 1/R$ . To account for the larger mass of the N—H group compared to hydrogen, the value of  $\nu_0$  for the reaction leading to the NH structure has been scaled with the square root of the respective mass ratio. The estimated hopping times for three different temperatures are given in Table III. Obviously, the energy barriers leading to the interface structures HD and NH can easily be overcome already at low temperatures. The CN2 structure, on the other hand, hardly forms at room temperature. Annealing will facilitate the hydrogen diffusion on the Si(001) surface and thus increase the possibility of forming structure CN2. At the same time, however, it will lead to an increased hydrogen desorption, and thus promote the formation of CN1.

### 3. Electronic properties

The influence of pyrrole adsorption on the density of surface states for energies around the fundamental band gap of

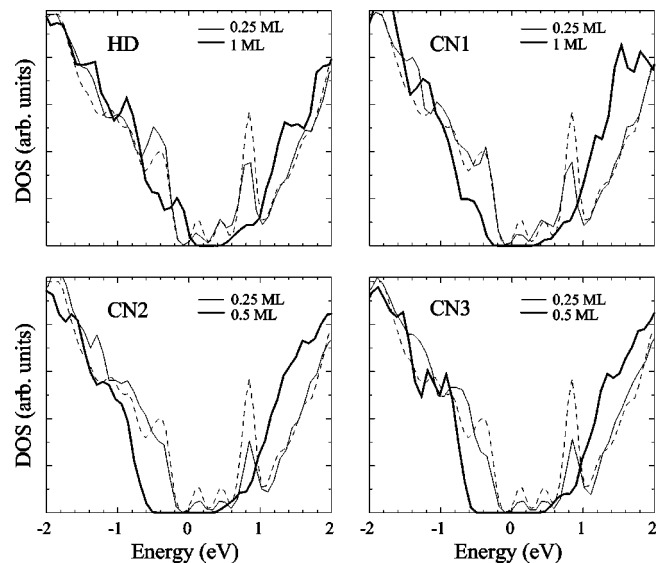


FIG. 7. Density of surface states around the fundamental band gap of Si for four structural models of Fig. 2. For comparison, the spectra of the clean Si(001) $c(4 \times 2)$  surface are shown by dashed lines.

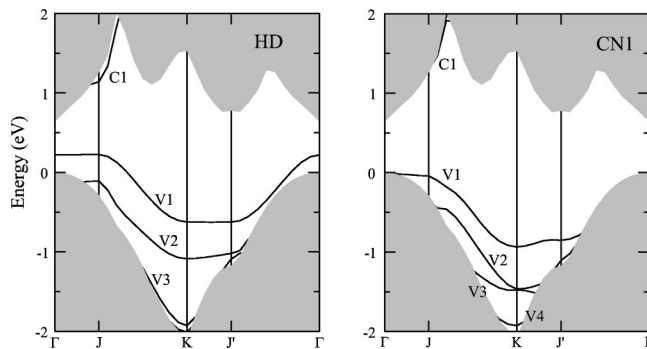


FIG. 8. Surface band structures (bound states) for the chemisorption structures HD and CN1. Grey regions indicate the projected bulk bands.

Si is shown in Fig. 7. We find that pyrrole adsorption leads to an efficient surface passivation, irrespective of the details of the adsorption geometry. Within DFT-GGA, a surface band gap of about 0.5 eV opens. This is the result of the saturation of the Si dimer dangling bonds by either N, C, or H. Consequently, the occupied/unoccupied Si surface state with partial  $\pi/\pi^*$  character localized at the “up”/“down” Si dimer atom is removed from the energy region of the Si bulk band gap.

The highest occupied surface state V1 for the HD and CN1 structures occurs around the Si bulk valence-band maximum, which is given by the energy zero in the surface band structures in Fig. 8. It is mainly localized at the chemisorbed pyrrole molecule (cf. Fig. 9) and can thus be considered as surface modified HOMO state. It is characterized by carbon-localized  $\pi$  orbitals. The relatively strong energy dispersion of this state is due to the interaction with the neighboring molecules. The surface states V2, V3, and V4, energetically below the valence-band maximum, have some

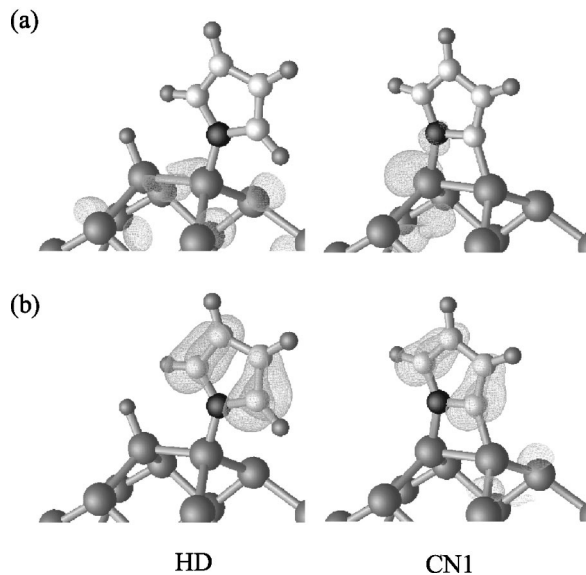


FIG. 9. Calculated charge-density plots (isosurfaces  $\rho = 0.05e/\text{\AA}^3$ ) for the surface localized states C1 and V1 of the HD and the CN1 structure are shown in (a) and (b), respectively (cf. calculated band structures in Fig. 8).

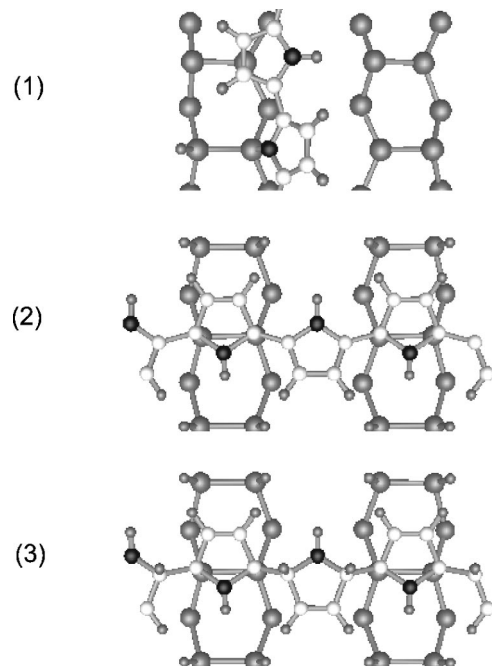


FIG. 10. Optimized geometries for the Si(001):polypyrrole interface. Black (white, grey) balls represent N (C, Si) atoms. Hydrogens are indicated by small symbols.

contributions from the pyrrole molecule, but are mainly derived from Si bonding states in the uppermost atomic layers. The lowest unoccupied state, C1, is nearly entirely formed by wave functions in the uppermost Si surface layers (cf. Fig. 9). The pyrrole LUMO state is energetically far above the Si bulk band gap, as can be expected from the HOMO-LUMO gap of 4.34 eV calculated for the gas-phase molecule.

The energetically favored interface structures HD, CN1, and CN2 preserve the aromaticity of pyrrole, in accord with the experimental findings of Cao *et al.*<sup>13</sup> They fulfill Hückel's criterion for aromaticity:<sup>33</sup> the formation of a closed loop of  $(4n+2)$   $\pi$  electrons with  $n$  being a positive integer (0,1,2, . . .).

### B. Polypyrrole on Si(001)

Several bonding configurations appear plausible for the adsorption of polypyrrole (PPy) chains on the Si(001) surface. The number of structural degrees of freedom is further increased, if additional hydrogen atoms are allowed to bond to the surface. The three energetically most favored structures among the ten geometries investigated in the present study are shown in Fig. 10. In all cases, the five-membered rings are arranged in an alternating fashion along the polymer chain. Adsorption models, where all rings point in the same position are energetically less favored. In model (1) (Fig. 10, the PPy chains are oriented parallel to the Si dimer rows, with their N atoms bonded to the Si dimer. The hydrogen atoms released upon PPy adsorption saturate the remaining Si dimer atoms. In models (2) and (3) the chains are oriented perpendicular to the Si dimer rows. They attach via

a Diels-Alder reaction to the substrate Si dimers. In model (3), additional hydrogen saturates the links between the polymerized pyrrole units.

The adsorption energy of model (1) amounts to 1.58 eV per two-ring PPy subunit for a coverage of 0.5 ML. Increasing the coverage to 1 ML yields a slightly smaller adsorption energy of 1.44 eV, indicating the repulsive interaction between the adsorbed polymer chains. For PPy model (2) an adsorption energy of 0.16 eV is obtained. The adsorption energy per poly(pyrrole 3-pyrroline) subunit is 0.95 eV for model (3).

The total energies of the PPy models (1) and (3) can directly be compared with the values calculated for the pyrrole structures CN1 and HD, respectively, because they have the same stoichiometry. For 0.5/1.0 ML coverage, the model (1) is less stable than the CN1 structure by 0.7/0.6 eV per pyrrole unit. The energy difference between the model (3) and the HD structure is even larger, 1.2 eV for full monolayer coverage. If both pyrrole and PPy compete for bonding sites on the Si(001) surface, no stable ordered PPy overlayer will form. Because of the different stoichiometry, the stability of the PPy model (2) can only be assessed using the calculated surface phase diagram of the hydrogen- and PPy-exposed Si(001) surface in Fig. 11. As can be seen, only in a hydrogen-poor environment, the PPy structure (1) may form. The models (2) and (3) are stable only for very high values of the PPy chemical potential and should not correspond to an equilibrium situation which can be realized experimentally. The overall instability of the PPy functionalized Si(001) surface can be understood from the lattice mismatch between PPy and silicon. According to the calculations, the PPy chains need to be stretched by about 7% in order to fit the Si(001) surface. The interface energetics may change, however, if the PPy chains are chemically modified, e.g., by doping.<sup>34</sup>

#### IV. SUMMARY

*First-principles* pseudopotential calculations for a large number of plausible Si(001):pyrrole and polypyrrole interface configurations are presented. We find dissociative reactions, leading to the partial fragmentation of the molecule, to be energetically most favored for pyrrole adsorption. The lowest energy configuration for monolayer coverage is char-

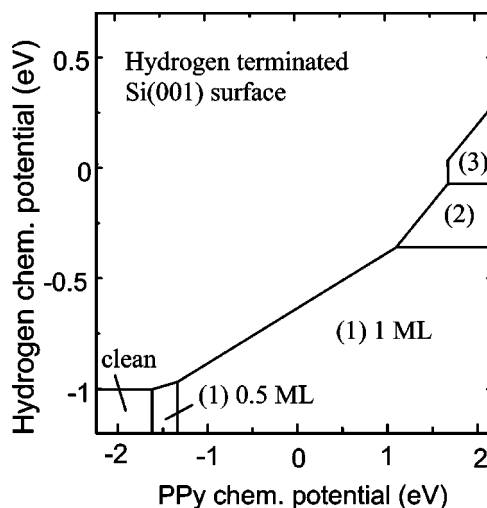


FIG. 11. Calculated phase diagram of the hydrogen- and polypyrrole-exposed Si(001) surface. The structural models (1), (2), and (3) are shown in Fig. 10. The chemical potentials of hydrogen and PPy are given with respect to molecular hydrogen and gas-phase PPy at  $T=0$ .

acterized by pyrrole rings bonded to the surface via Si—N linkage. For a low coverage of pyrrole molecules or a hydrogen-poor environment, adsorption geometries where both N and C are bonded to the surface are energetically favored. The energetically favored interface structures retain the aromaticity of the pyrrole molecule. The co-existence of these geometries accounts very well for the available experimental data. The chemisorption of pyrrole is found to effectively passivate the Si(001) surface, irrespective of the details of the adsorption geometry. The formation of well-ordered polypyrrole structures on Si(001) may require chemical modifications of the polypyrrole chains in order to account for the lattice mismatch.

#### ACKNOWLEDGMENTS

Grants of computer time from the Leibniz-Rechenzentrum München, the Höchstleistungs-Rechenzentrum Stuttgart, and the John von Neumann-Institut Jülich are gratefully acknowledged.

\*Electronic address: seino@ifto.physik.uni-jena.de

<sup>1</sup>R. A. Wolkow, *Annu. Rev. Phys. Chem.* **50**, 413 (1999).

<sup>2</sup>R. J. Hamers, *Nature (London)* **412**, 489 (2001).

<sup>3</sup>S. F. Bent, *Surf. Sci.* **500**, 879 (2002).

<sup>4</sup>U. Birkenheuer, U. Gutdeutsch, and N. Rösch, *Surf. Sci.* **409**, 213 (1998).

<sup>5</sup>P. L. Silvestrelli, F. Ancilotto, and F. Toigo, *Phys. Rev. B* **62**, 1596 (2000).

<sup>6</sup>W. A. Hofer, A. J. Fisher, G. P. Lopinski, and R. A. Wolkow, *Phys. Rev. B* **63**, 085314 (2001).

<sup>7</sup>Y. Morikawa, *Phys. Rev. B* **63**, 033405 (2001).

<sup>8</sup>W. Kim, H. Kim, G. Lee, Y.-K. Hong, K. Lee, C. Hwang, D.-H. Kim, and J.-Y. Koo, *Phys. Rev. B* **64**, 193313 (2001).

<sup>9</sup>J.-H. Cho and L. Kleinman, *Phys. Rev. B* **64**, 235420 (2001).

<sup>10</sup>W. Lu, W. G. Schmidt, and J. Bernholc (unpublished).

<sup>11</sup>Z. Lin, T. Strother, W. Cai, X. Cao, L. M. Smith, and R. J. Hamers, *Langmuir* **18**, 788 (2002).

<sup>12</sup>M. H. Qiao, Y. Cao, J. F. Deng, and G. Q. Xu, *Chem. Phys. Lett.* **325**, 508 (2000).

<sup>13</sup>X. Cao, S. K. Coulter, M. D. Ellison, H. Liu, J. Liu, and R. J. Hamers, *J. Phys. Chem. B* **105**, 3759 (2001).

<sup>14</sup>H. Luo and M. C. Lin, *Chem. Phys. Lett.* **343**, 219 (2001).

<sup>15</sup>L. H. Sperling, *Introduction to Physical Polymer Science* (John Wiley & Sons, New York, 1992).

<sup>16</sup>Y. Okawa and M. Aono, *Nature (London)* **409**, 683 (2001).

<sup>17</sup>T. Livache, B. Fouque, A. Roget, J. Marchand, G. Bidan, R. Té-

- oule, and G. Mathis, *Anal. Biochem.* **255**, 188 (1998).
- <sup>18</sup>G. Kresse and J. Furthmüller, *Comput. Mater. Sci.* **6**, 15 (1996).
- <sup>19</sup>J. P. Perdew, J. A. Chevary, S. H. Vosko, K. A. Jackson, M. R. Pederson, D. J. Singh, and C. Fiolhais, *Phys. Rev. B* **46**, 6671 (1992).
- <sup>20</sup>J. Furthmüller, P. Käckell, F. Bechstedt, and G. Kresse, *Phys. Rev. B* **61**, 4576 (2000).
- <sup>21</sup>J. L. Brédas, R. Silbey, D. S. Boudreaux, and R. R. Chance, *J. Am. Chem. Soc.* **105**, 6555 (1983), and references therein.
- <sup>22</sup>*Semiconductors: Physics of Group IV Elements and III-V Compounds*, edited by O. Madelung, Landolt-Börnstein, New Series, Group III, Vol. 17, Pt. a (Springer-Verlag, Berlin, 1991).
- <sup>23</sup>*CRC Handbook of Chemistry and Physics*, edited by D. R. Lide, 79th ed. (CRC Press, Boca Raton, 1998-1999).
- <sup>24</sup>P. Pulay, *Chem. Phys. Lett.* **73**, 393 (1980).
- <sup>25</sup>D. M. Wood and A. Zunger, *J. Phys. A* **18**, 1343 (1985).
- <sup>26</sup>K. Seino, W. G. Schmidt, J. Furthmüller, and F. Bechstedt, *Surf. Sci.* (to be published).
- <sup>27</sup>M. H. Qiao, F. Tao, Y. Cao, Z. H. Li, W. L. Dai, J. F. Deng, and G. Q. Xu, *J. Chem. Phys.* **114**, 2766 (2001).
- <sup>28</sup>G.-X. Qian, R. M. Martin, and D. J. Chadi, *Phys. Rev. B* **38**, 7649 (1988).
- <sup>29</sup>C. G. Van de Walle and J. Neugebauer, *Phys. Rev. Lett.* **88**, 066103 (2002).
- <sup>30</sup>R. Miotto, G. P. Srivastava, R. H. Miwa, and A. C. Ferraz, *J. Chem. Phys.* **114**, 9549 (2001).
- <sup>31</sup>E. Penev, P. Kratzer, and M. Scheffler, *J. Chem. Phys.* **110**, 3986 (1999).
- <sup>32</sup>D. R. Bowler, J. H. G. Owen, K. Miki, and G. A. D. Briggs, *Phys. Rev. B* **57**, 8790 (1998).
- <sup>33</sup>W. H. Brown and C. S. Foote, *Organic Chemistry* (third edition) (Harcourt College Publishers, Fort Worth, 2002).
- <sup>34</sup>A. J. Heeger, *Rev. Mod. Phys.* **73**, 681 (2001).